РОССИЙСКАЯ АКАДЕМИЯ НАУК

Физический институт имени П.Н.Лебедева

Ф И А Н

PREPRINT

13

Yu.A. MIKHAILOV, L.A. NIKITINA,
G.V. SKLIZKOV, A.N. STARODUB,
M.A. ZHUROVICH

RELATIVISTIC ELECTRON HEATING IN FOCUSED MULTIMODE LASER FIELDS WITH STOCHASTIC PHASE PERTURBATION

MOSCOW 2007

Нагрев релятивистских электронов в лазерном поле со стохастическими возмущениями фазы

Ю.А.Михайлов, Л.А.Никитина, Г.В.Склизков, А.Н.Стародуб, А.Журович
Физический институт им. П.Н.Лебедева РАН, Ленинский пр-т, 53, Москва

Абстракт

Рассматривается численная модель прямого ускорения релятивистских электронов в заданном электромагнитном поле. Источником случайных сил является фазово неоднородное поле в фокусе многомодового лазерного пучка со стохастическими пространственно временными неоднородностями фазы для каждой спектральной компоненты. Энергия электронов превышает 10 МэВ даже при умеренных плотностях потока $\sim 10^{16}$ Ватт/см^2. Разработанная программа позволяет получить количественно энергетическую функцию распределения в зависимости как от интенсивности поля, так и от длительности импульса параболической формы. Эффективный нагрев электронов происходит в присутствии встречной волны, отраженной от критической области при заданном коэффициенте отражения. Стохастический нагрев происходит с задержкой относительно начала лазерного импульса, когда лазерные поля превысят некоторые пороговые амплитуды. Для иллюстрации справедливости предлагаемого механизма ускорения приведено качественное сравнение результатов моделирования с экспериментальными данными.

Relativistic Electron Heating in Focused Multimode Laser Fields with Stochastic Phase Perturbations[1]

Yu.A.Mikhailov, L.A.Nikitina, G.V.Sklizkov, A.N.Starodub, M.A.Zhurovich
P.N.Lebedev Physical Institute of RAS, Leninsky pr 53, Moscow

Abstract

A direct relativistic electron acceleration simulation model with a given electromagnetic field, which is determined by the wave packet parameters, is considered. The multimode time-spatial structure of a focused Nd-laser beam with stochastic phase disturbances of each of the spectral components is taken into account as a source of random forces. The electron energies of more than 10 MeV are derived even at moderate flux densities of 10^{16} W/cm^2. The developed numerical code makes it possible to obtain a quantitative energy distribution function in relation to both the field intensities and temporal U-shape of the laser pulse. An efficient heating of electrons can be triggered in the presence of counter propagating wave being reflected from the critical plasma area with varied reflection coefficient. The heating mechanism occurs with a delay relative to the beginning of a pulse when the laser fields exceed certain threshold amplitudes. A qualitative comparison of simulation results with the experimental data is given as the evidence that this mechanism is not unreasonable.

---

[1] Text of the report presented to 3rd International Conference on the Frontiers of Plasma Physics and Technology (FPPT-3), March 5-9, 2007, Bangkok, Thailand.

1. Introduction

Generation in the laser plasma of the electrons with an energy many times greater than that of the thermalized electrons is an extremely important physical phenomenon. Study of the generation and acceleration of fast electrons in the laser plasma makes it possible to understand and investigate some complicated physical processes that can accelerate the electrons to very high energies. The examples of such processes are the resonant absorption of laser radiation in plasma and the parametric instabilities near the critical density, the two-plasmon decay in the region of quarter-critical density, the stimulated Raman scattering in plasma coronas, and the discussed here relativistic electron heating in the focused multimode laser fields with stochastic phase perturbations. From the practical point of view, it is very promising to use the laser plasma, which generates fast electrons, as the cathode of an injector of high-current pulsed accelerators since such laser-plasma cathodes can, as compared with traditional types of the cathodes, ensure high initial energy of electrons ($>10^2$ keV), a short duration of the injection pulse ($<10^{-9}$ s), and huge current densities ($>10^6$ A/cm^2). The generation of fast electrons in the laser plasma can play a very important role for the purposes of laser thermonuclear fusion. In the schemes of hydrodynamic acceleration and compression of thermonuclear targets, even a small number of high-energy electrons carry less than 1% of the absorbed laser energy penetrating into the central region of the target. This can cause the preheating and, thereby, catastrophically lower the compression by more than an order of magnitude and prevent the attainment of a necessary value of the confinement parameter ρR (ρ, $R-$ are the density and radius core of a target). On the other hand, in the currently widely discussed promising scheme of laser thermonuclear fusion known as "fast ignition", one of the decisive factors in achieving success is the possibility to generate in the coronal region of the thermonuclear target the high-energy electrons under the influence of an ultrashort pulse of laser radiation in order to

ensure effective transport of energy via these electrons into the ignition region. In many experimental works the superthermal electrons have been observed. The presence of hot electrons resulted in the appearance of high energetic ions and anomalously hard X-ray emission spectrum. The most recent papers, which deal with hot electron observation are concerned with laser plasma produced by femtosecond laser radiation focused onto a solid target at flux densities of $10^{18}-10^{20} W/cm^2$. The relativistic factor is much more than unity at such radiation densities. There are few experiments in the range of $10^{13}-10^{15} W/cm^2$ and at nanosecond pulse duration, in which the anomalously energetic electrons (essentially more than oscillatory energy) have been registered. The most important is the fact that a significantly large part of incident laser energy was converted into the energy of hot electrons. In a number of works different stochastic acceleration mechanisms have been considered to explain anomalous energy of electrons. Here the spontaneous self-generated magnetic fields or plasma wave beating or the wake fields were used as a source of random perturbation of momentum of an electron. See, for example, [1-4]. The laser energy transfer and the enhancement of plasma waves and electron beams by the interfering in high-intensity laser pulses were considered in [5].

In the present paper, we consider a mechanism of stochastic electron heating under critical homogeneous electron density and at focal intensities in the range of $10^{13}-10^{17} W/cm^2$, which are important for direct fusion target heating. The field random phase distribution over the focal plane (speckle structure of intensity), as well as the phase beating in the wave packet of multi-mode Nd-laser beam of 3ps duration, are taken into account as a source of random forces in the equation of motion of a charged particle. The dependence of electron energy distribution function shape and dependence of the mean energy on the focal intensity was obtained numerically. The calculation of

trajectories of 2000 electrons showed the directivity at an output equal to $\sim 0.7\,rad$. The wave reflected from critical area was taken into account.

2. Intensity and field distribution in the focal plane

The focal intensity distribution was measured for an aspherical lens with the focus of 10 cm and aperture of the beam of 45 mm. The laser beam energy was 20 J and nanosecond pulse duration. Then we reconstruct the field distribution numerically by choosing the structure of the beam, which corresponds to the focal intensity. We use an angle structure consisting of several tens of angular modes, so the total divergence was about $\sim 2 \cdot 10^{-4}\,rad$. In Figures. 1 and 2 the typical intensity and field distributions are given for a focal Y-Z plane.

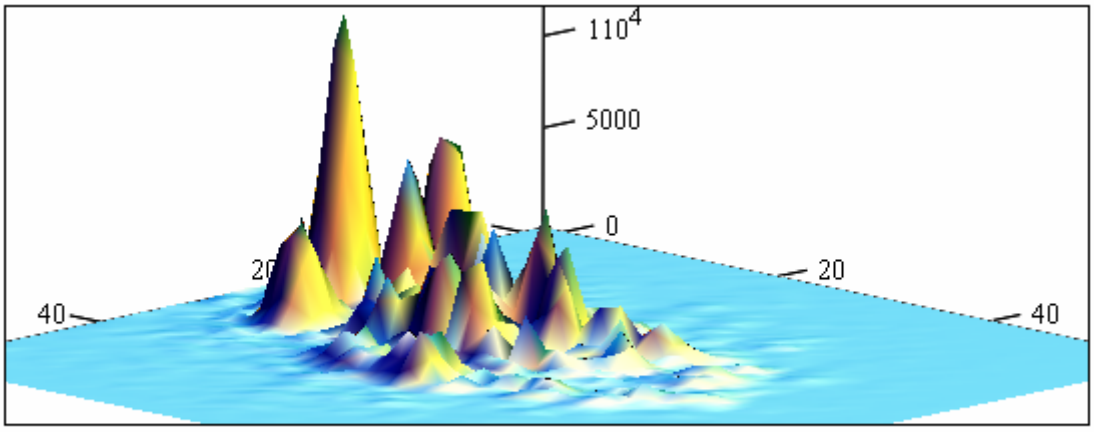

Fig.1. Typical focal intensity distribution.

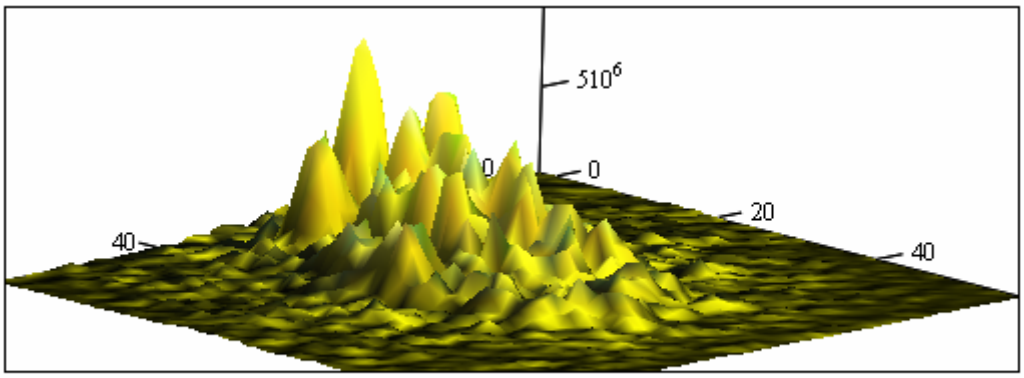

Fig.2. Typical field intensity distribution.

Polarized *E*-field phase distribution is shown in Figures 3 and 4.

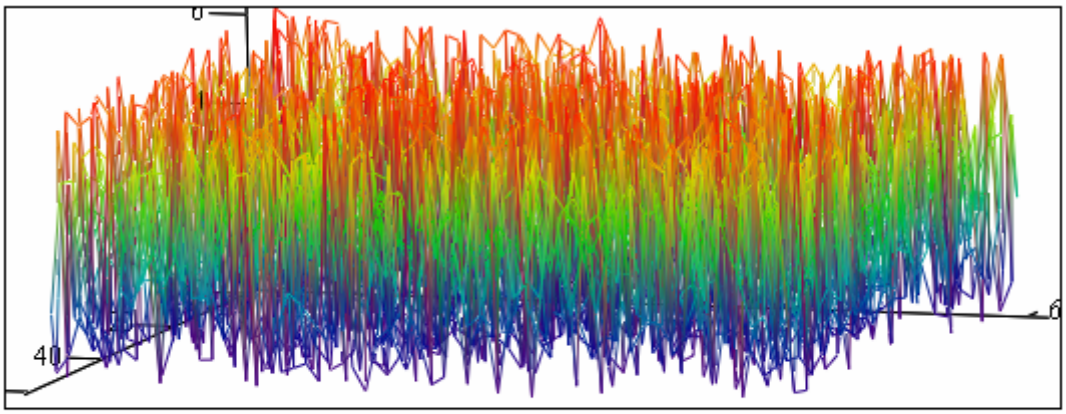

Fig.3. Electric field phase distribution over the focal Y-Z plane.

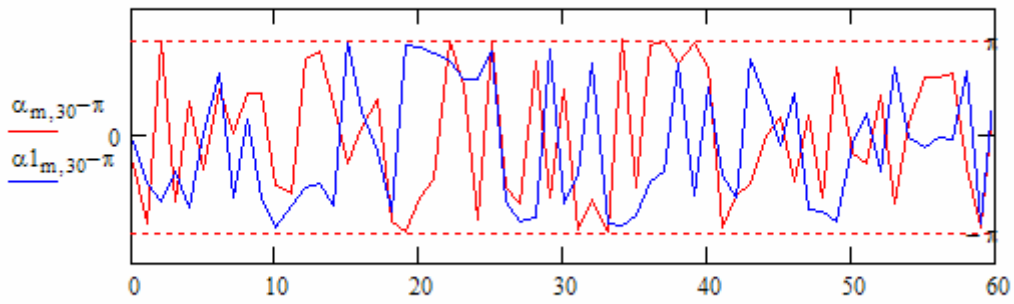

Fig.4. Field phase traces in two perpendicular directions over the focal plane.

Here are the field phase traces for two perpendicular crossections, $y=0$, or $z=0$. Note, that the phase randomly changes from π to minus π over the Y-Z plane. The relative phase shift between two successive maxima or minima of the R-field is shown. An absolute phase shift therewith is defined with the accuracy $2\pi n$, where $n-$ is integer.

3. The model

The model describes the acceleration of charged test particles in a given electromagnetic field formed in the focal area by the polarized incident and reflected light beams. The incident and reflected beams consist of several frequency components each. A complicated phase structure of the focal intensity speckle patterns was approximated by regular phase perturbation in time with random phase shock amplitude. The frequency of phase shocks, which the electron meets along the motion trajectory, corresponds to 2/3 of the critical plasma frequency. A moving electron experiences an electromagnetic field the phase of which changes sharply in a time rather less than the wavelength period. Then the phase is constant until the next phase jump occurs. The random spread of relative phase of each of the spectral components was taken into account. The temporal shape of the laser beam wave packet was the U-shape, which is approximated by an envelope function $\delta(t)=\left[\left(1-\frac{t}{\tau}\right)\cdot\frac{t}{\tau}\right]$. The multi component spectral line of laser radiation approximated by the function $f(j)=\left(1-\frac{j}{N_L}\right)\cdot\frac{j}{N_L}$, where $j-$is the component number, N_L-, the number of components. For example, the Nd-glass radiation usually consists of twelve spectral components. However, in this paper we consider only four components to simplify and quicken numerical procedure. The phase factor of a component is given by expression

$$f_e(j,t)=\exp\left(i\cdot\left[\omega_0\left[1+\left(\frac{\Delta n_\lambda}{n_\lambda}\right)\cdot\left(j-\frac{N_L}{2}\right)\right]\cdot\left(t-\frac{\tau}{2}\right)-\Phi_j\right]\right)\cdot f(j),$$

where ω_0 – is the frequency at the maximum of spectral line; n_λ – the number of periods in pulse duration τ; Δn_λ – the frequency interval in a number of periods between the neighboring equidistant spectral components; Φ_j – the random phase (but not more than it follows from uncertainty condition). For example, in the case of a polarized field we can write

$$E_y(\vec{r},t)=A(y,z)\cdot\left(\sum_{j=0}^{N_L} f_e(j,t)\right)\cdot\left[(1-\gamma)\cdot e^{-ik_x x}+2\gamma\cos k_x x\right]\cdot\delta(t)e^{i\psi(t)},$$

$$H_z(\vec{r},t)=A(y,z)\cdot\left(\sum_{j=0}^{N_L} f_e(j,t)\right)\cdot\left[(1-\gamma)\cdot e^{-ik_x x}-2i\gamma\sin k_x x\right]\cdot\delta(t)e^{i\psi(t)},$$

where $k_x\approx\frac{2\pi}{\lambda}$ - is the wave number; $\psi(t)$– the random function; $\gamma=\frac{E_{refl}}{E_{inc}}$ the amplitude reflection coefficient. The longitudinal and depolarization parts of the fields are written in a similar way. They do not influence essentially the electron stochastic motion, at least at the level of 20% of field amplitude. In our model the spatial non-uniformity of the field does not strongly influence the energy gain in contrast to [6].

4. Stochastic Equations of Motion

To investigate the acceleration of test particles in the electromagnetic fields formed as described above, we consider the relativistic equations of motion of a positive electron in a given external electromagnetic field:

$$\frac{d\bar{r}'}{dt'}=v'(\bar{p}');\qquad\qquad \frac{d\bar{p}'}{dt'}=\frac{q}{c}\cdot\bar{v}'(\bar{p}')\times\bar{B}(\bar{r}',t')+q\cdot\bar{E}'.$$

Here the variables p'_X, p'_Y, p'_Z, x, y, z are the unknown ones; the dotted values relate to the real ones. For the numerical integration, we express equations in terms of the following relations: $t = ct'$, $\vec{p} = \frac{\vec{p}'c}{mc^2}$, $T_{kin} = \frac{T'_{kin}}{mc^2}$, $\vec{V} = \frac{\vec{V}'}{c}$, $E = \frac{qE'}{mc^2}$, $B = \frac{qB'}{mc^2}$. Now we write the reduced equations in the form:

$$\begin{cases} \frac{d\vec{r}}{dt} = \vec{\beta}(\vec{p}), \qquad \vec{\beta}(\vec{p}) = \frac{\vec{p}}{\sqrt{1+(\vec{p}\cdot\vec{p})}}, \\ \frac{d\vec{p}}{dt} = \vec{\beta}(\vec{p}) \times \vec{B}(\vec{r},t) + \vec{E}(\vec{r},t). \end{cases}$$

Here time t is expressed in cm. The coordinates x, y, z in cm are unchangeable. The reduced energy T and momentum p_x, p_y, p_z assigned in units of electron rest energy mc^2. The particle motion equations are solved with a 4th order Runge-Kutta adaptive step-size scheme. In numerical calculations we analyze the motion of 1000-2000 free electrons. The laser pulse duration is ~3.5 ps, and is appropriate to 1000 wavelengths. The pulse shape was approximated by parabolic function $\delta(t)$ with a high contrast ratio, which is rather different from the Gaussian shape. The electrons gain the most part of energy only in the X-Y plane in spite of a 3D trajectory. We consider a uniform neutral cloud of non-interacting electrons in spatially and time modulated electromagnetic field. The test electrons start to accelerate within the simulation box at random positions. The momentum initial conditions corresponded to normal distribution with the temperature of ~0.5 keV, and represented a typical value in laser plasma corona near critical area for focal intensities under consideration. The simulations were performed with a resolution of 50 cells per laser wavelength and the time step was carefully chosen to ensure that the numerical dispersion did not influence the results.

5. The Electron Trajectories

In Figure 5 a set of trajectories projected onto the X-Y plane of typical test electron is shown. The end of a trajectory is consistent with the end of the wave packet subsequent to electromagnetic fields are switched off. One can see that during irregular motion the particle is subjected to a random force, and the lower is the momentum the stronger is the force. When a stochastic acceleration is developed the motion of the particles becomes directional. Most electrons move in the direction of incident wave propagation. It is noticeable that about half of the particles move inside an angle of ~0.7 rad (for 2000 particle trajectory analysis). In the case of long pulses of 3.5 ps and 10 ps duration the directivity of particle motion does not depend on the initial phase position, i.e. on the random initial position in simulation box. The same regards to random initial energy of a particle. This fact confirms the stochastic nature of motion under electromagnetic field phase perturbation. In this case the electric field E_y and the magnetic field B_z were polarized. The longitudinal components of the electromagnetic fields were not taken into account. Small depolarization ~5% does not strongly influence the trajectories. Each incident field consists of two frequency components with frequency interval $\Delta\omega = \omega_0/500$ and a random relative phase. The reflection coefficient was equal to $\gamma = 0.2$. When reflection is close to unity, $\gamma > 0.8$ The electron motion reminds one of the case of a standing wave. The directivity of electron motion to the end of the pulse therewith becomes almost isotropic.

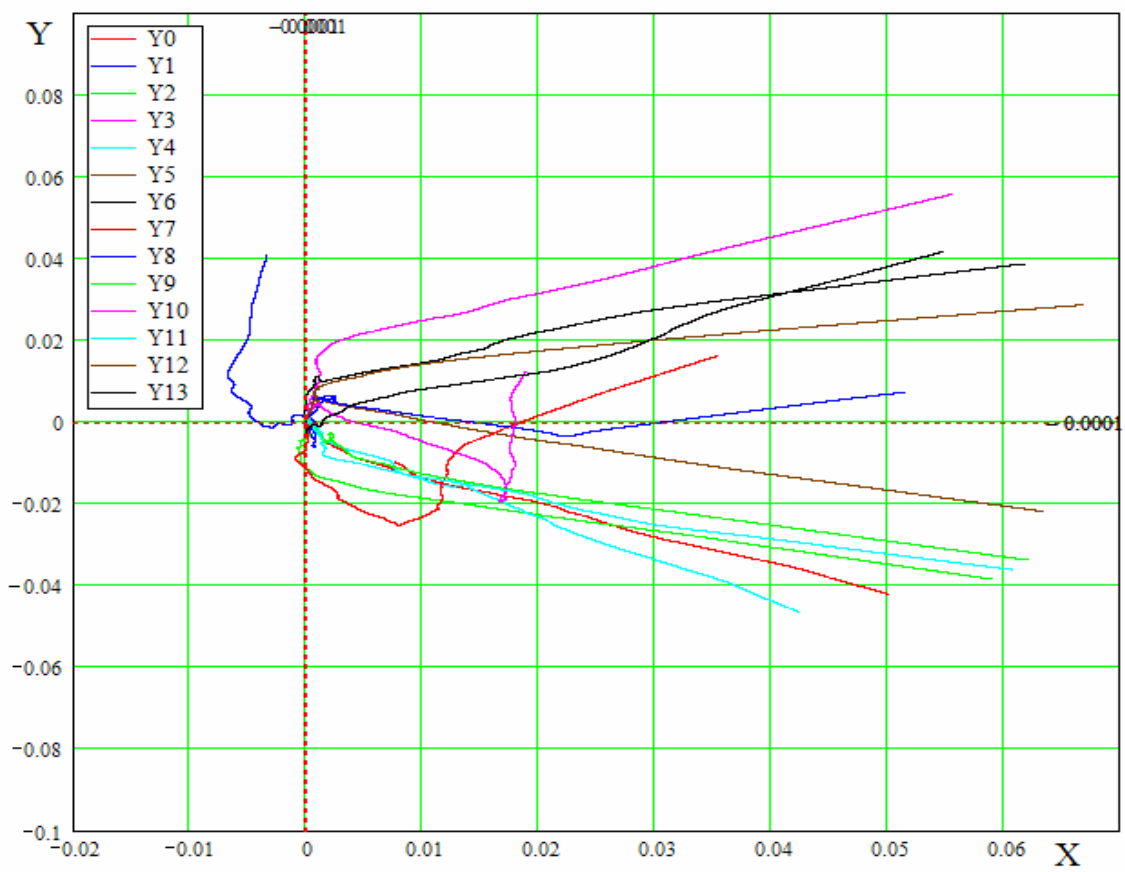

Fig. 5. Trajectories projected on to X-Y plane for typical test electrons. X [cm] is parallel to wave vector $\vec{k}$; Y [cm] parallel to *E*. The fourteen curves are taken arbitrarily.

In Figure 6 the early stage of particle acceleration is shown. One can easily see that the initial stage of motion of the particle is strongly dependent on the random initial energy and space phase position in simulation box. However, at the early times that is a few tens of wave periods the increase of stochastic energy of a particle is not noticeable. The direction of initial particle moving is dependent on random initial phase and the values of momentum components. In some cases a long linear part of trajectory can be seen that implies to the minimum of magnetic field in the point of initial position of a test particle.

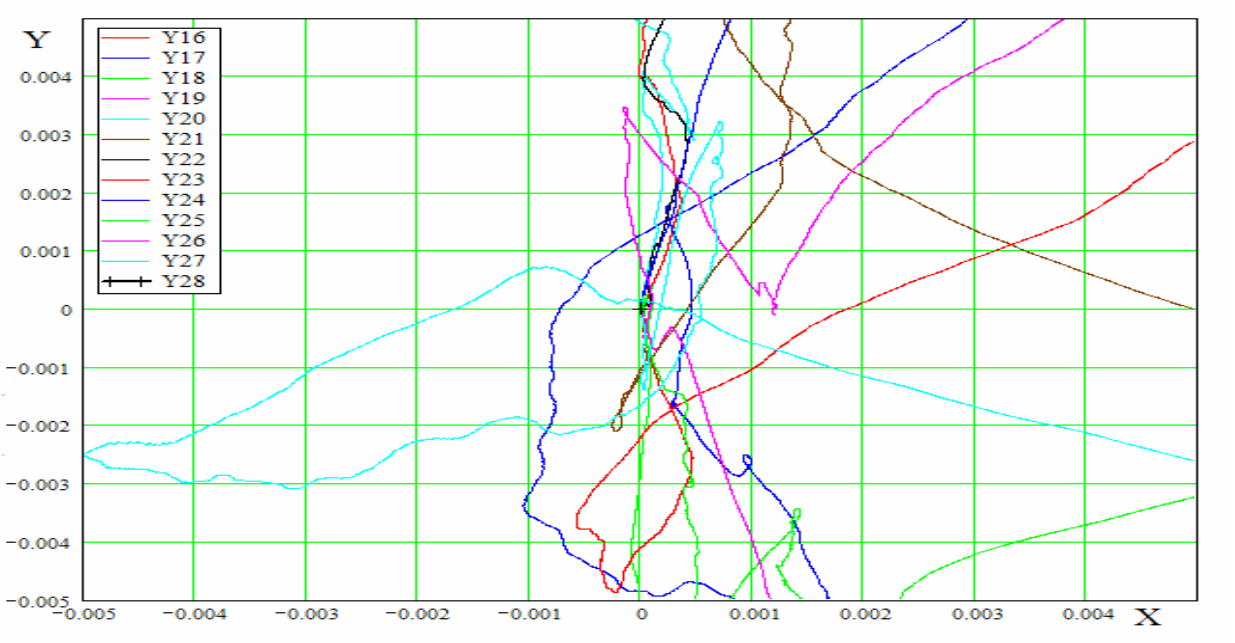

Fig.6. The early stage of particle trajectories X [cm] is parallel to K; Y [cm] parallel to E.

6. The energy gain of a particle during the laser pulse

In Figure 7 the time evolution of the kinetic energy of a test electron for a fixed field intensity corresponding to the light intensity $q = 2 \cdot 10^{17}\, W/cm^2$ is shown. There are typical fifteen randomly selected traces from 1000 ones. The initial conditions are as mentioned above. The time [in cm] is plotted on X-axis. A vertical division is equal to 10 MeV for each trace. The field is switched off at 0.1 cm for the convenience of observation. It is easily seen that a stochastic process of particle acceleration develops after the delay, which varies from tens to hundreds of wavelengths. This delay is longer than for the case of a rectangular pulse when the field is switched on instantaneously. The damping of small variations is related to the decrease of field intensity on the slope of the pulse. The small structure of an energy evolution trace come from the force perturbations, which result in the direction change of the momentum of a test particle.

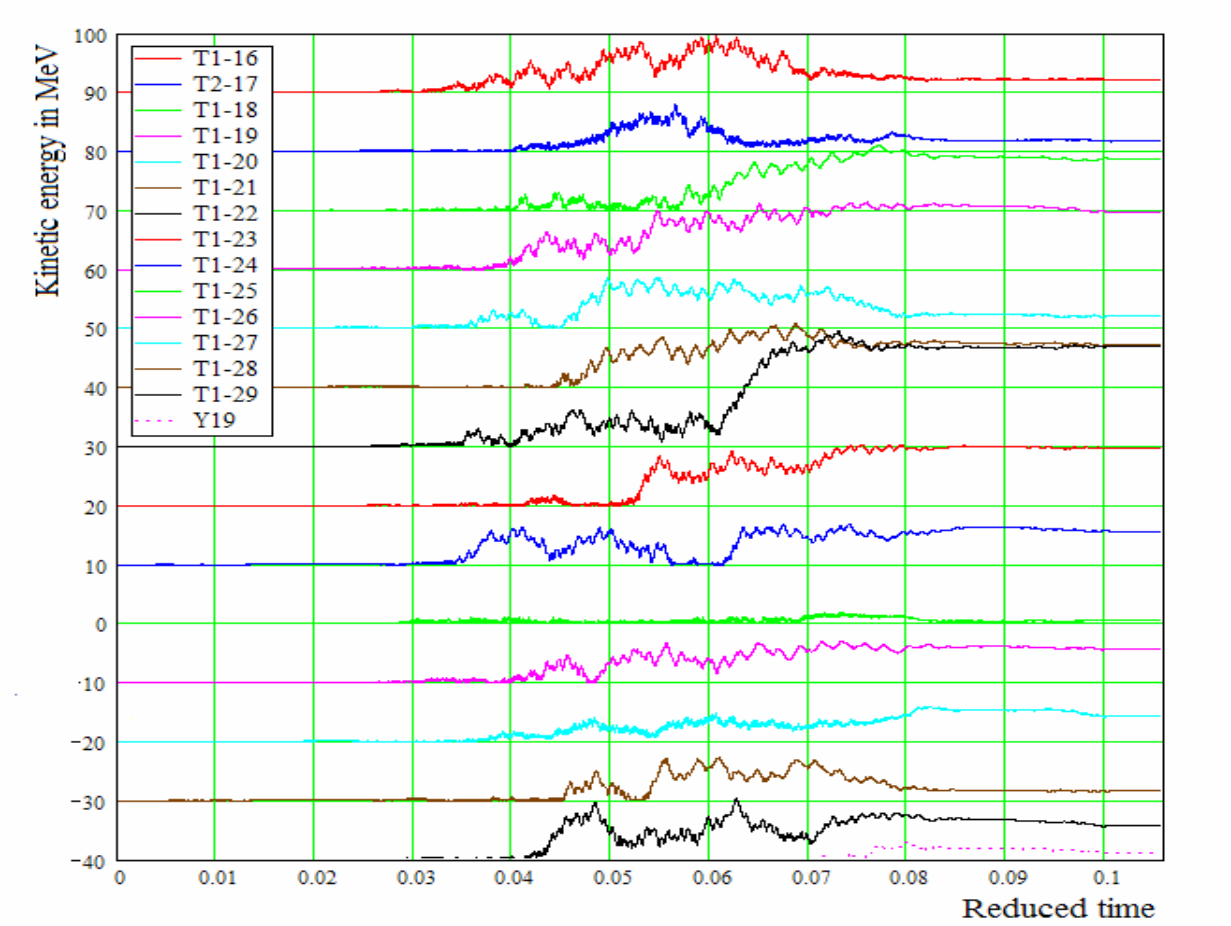

Fig.7. Time evolution of the kinetic energy of a test electron for fixed field intensity corresponded to the light intensity $q = 2 \cdot 10^{17}\, W/cm^2$. Each cell in a vertical axis is equal to 10 MeV for the corresponding curve. The pulse duration is 3.5 ps.

7. Energy Spectrum of Electrons

In Figure 8 the distribution functions of the electrons normalized to the maximum probability for different field intensities are presented. The figure denoted by "mean" implies to the energy averaged over a proper curve. The figure denoted by "max" implies to the energy related to the maximum energy of all the electrons, and the energy of each electron is averaged over the time of field action. The parameter eb implies the value of field intensity in terms of Mega $CGSE/cm$. For example, $eb = 20$ is matched to power density of

$q = 10^{17}\, W/cm^2$. The parameter $eb = 0.5,\ 1,\ 2,\ 3,\ 4,\ 5,\ 10,\ 20$ in Figure 8 denotes the distribution functions corresponding to the field intensities equal to $6\cdot10^{13}$, $2.5\cdot10^{14}$, 10^{15}, $2\cdot10^{15}$, $4\cdot10^{15}$, $5.2\cdot10^{15}$, $2.5\cdot10^{16}$, 10^{17} W/cm^2. The energy distribution functions are not Maxwellian, they have a long energetic tail.

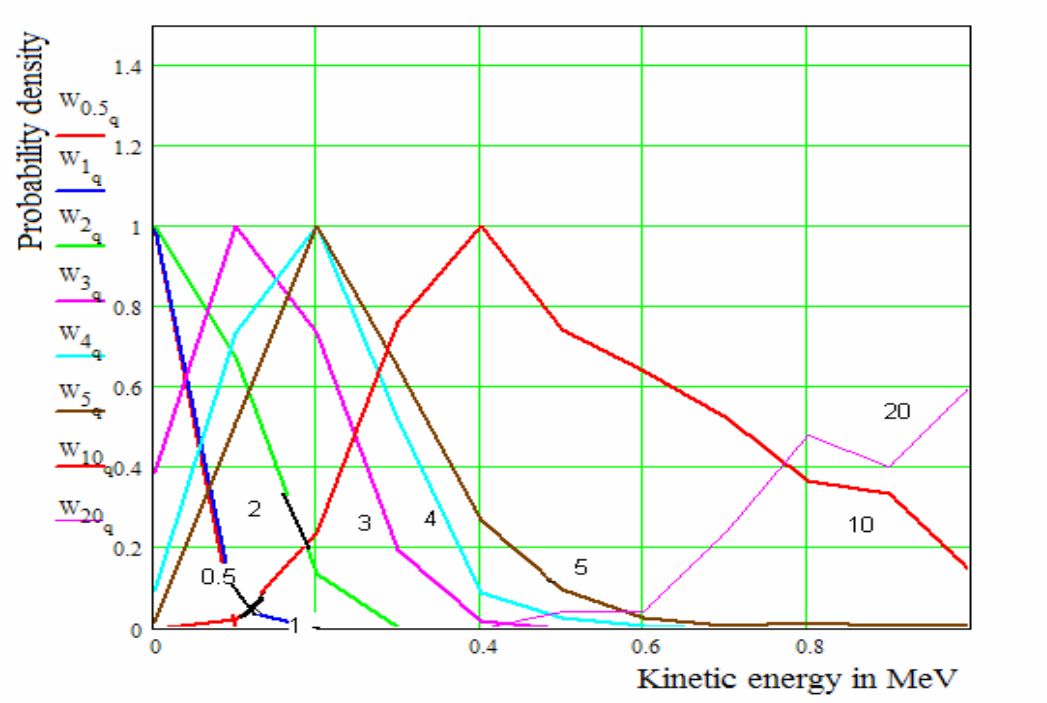

Fig.8. The distribution functions of electrons normalized to the maximum probability for different field intensities. The figures near the curves show the distribution functions corresponding to the field intensity parameter eb.

In Figure 9 the curves denoted the "output energy probability" correspond to the energy distribution functions of electrons at the end of the laser pulse of ~3.5 ps duration. The curves "cutoff energy probability" shows the fractional number of electrons having the energy more than in the corresponding figure on X-axis. The curves "cutoff current" show the normalized current, which can be registered by a detector outside the interaction area. It is seen from these graphs that at flux density of $10^{17}\, W/cm^2$ more than 20% of electrons can have the

energies higher than 6 MeV. Here "output energy probability" means the energy distribution of 1000 electrons at the time equals to 90% of the pulse duration. The "cutoff energy probability" means the fraction of particles having the energy, which exceeds the corresponding value on X-axis. The "cutoff current" means the fractional current value of electrons, which escapes the focal area and have the energy higher than the value on X-axis one. The parameter eb indicates the value of field intensity in units of $10^6\,CGSE = 3\cdot 10^8\,V/cm$. The dotted curves designated by "cutoff current" show the probability of total flow of particles, which escape the interaction area. It is really the electric current which can be measured like in the previous work at the intensities of $10^{13} \div 10^{15}\,W/cm^2$.

The curves "cutoff energy probability" show the fractional number of particles which have the energy higher than the energy at X-axis. At flux density of $q = 10^{17}\,W/cm^2$ $(eb = 20)$ the energy distribution function is not smooth and is not explained simply. We can only say that this is not associated with numerical procedure at least within the framework of approximation model given above. The data given in Figure 9 result in a large amount of electrons with the energy higher than relativistic oscillatory energy. For example, the fractional part of electrons which have the energies higher than 350 keV is equal to ~15% even at a relatively low intensity $\sim 6\cdot 10^{15}\,W/cm^2$, and the same 15% part of electrons have the energies higher than 2 MeV at the intensity of $\sim 2\cdot 10^{16}\,W/cm^2$. These curves were obtained by processing 2000 electron trajectories which were calculated with 80 cells per wavelength ($\lambda = 1.06\,\mu m$).

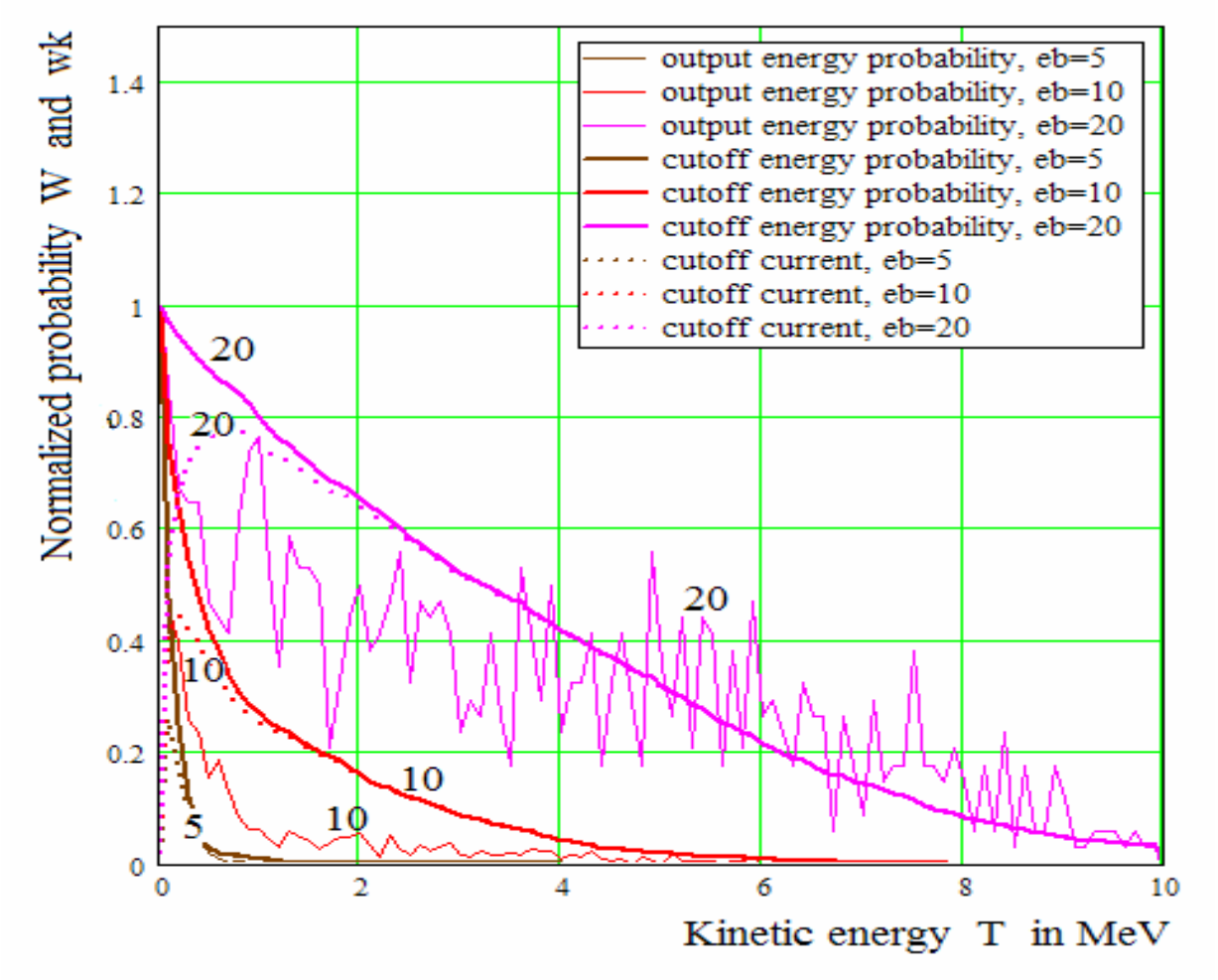

Fig.9. Energy distribution functions of electrons at the end of the laser pulse of ~3.53 ps duration.

8. The discussion

In Figure 10 we made an attempt to compare the simulation results and the experimental data. The points were obtained by measuring total cutoff electron current from a copper solid target. The cutoff current is expressed by $j_{cutoff} \sim \int_T^\infty w(T) \cdot \frac{\sqrt{T(T+2)}}{T+1} dT$, where $w(T)$ is the electron energy distribution function. Here the two boxes correspond to intensity of $\sim 10^{16} W/cm^2$ measured as the one averaged over the focal spot and in time.

Indeed there are the spikes of intensity several times higher than averaged intensity. So these points can be compared with the middle bold curve calculated at intensity of $2.5 \cdot 10^{16}\, W/cm^2$. The three diamonds were measured at focal intensity of $\sim 10^{14 \div 15}\, W/cm^2$. We try to comply these points with the lower bold curve calculated at the intensity of $6 \cdot 10^{15}\, W/cm^2$. The upper bold curve for the current was calculated at the intensity of $10^{17}\, W/cm^2$ $(eb = 20)$. This illustrates that half of the electrons gain the energy of more than 3 MeV. Qualitatively it is not contradictory to the results obtained experimentally with femtosecond pulses [2, 4]. However, a quantitative comparison is impossible. Nevertheless, the model in which the random phase perturbation of the focal field phase is taken into account can be considered to be a real possibility to explain the appearance of anomalously energetic electrons in the laser plasma at moderate intensity density. It is notable that up to 30% of absorbed laser energy was converted in electrons with mean energy exceeding 600 keV at 0.5 ps pulse duration, 15 J pulse energy, and intensity of $\sim 10^{19}\, W/cm^2$ [2], and up to 30% of absorbed laser energy was the energy of the target charge due to 300 keV electrons at 2 ns, $\sim 10^{14}\, W/cm^2$ and 3.53 ps, $\sim 10^{15}\, W/cm^2$ pulses [1].

The processing of the data obtained by simulation resulted in the dependence of electron energies on the focal laser power density, and this is consistent with our theoretical model. The four curves are shown in Figure 11 where in the X-axis the intensity and in the Y-axis the energy are plotted in absolute units. The upper curve (diamonds) shows the dependence of maximal energy on the intensity. The next lower curve (circles) shows the dependence of maximal energy on the intensity during the pulse averaged over 1000 electrons. The next lower curve (boxes) relates to the averaged energy of electrons at the end of the pulse. Finally, the lowest curve (crosses) relates to electron energy averaged over all electrons and averaged over the pulse for each electron.

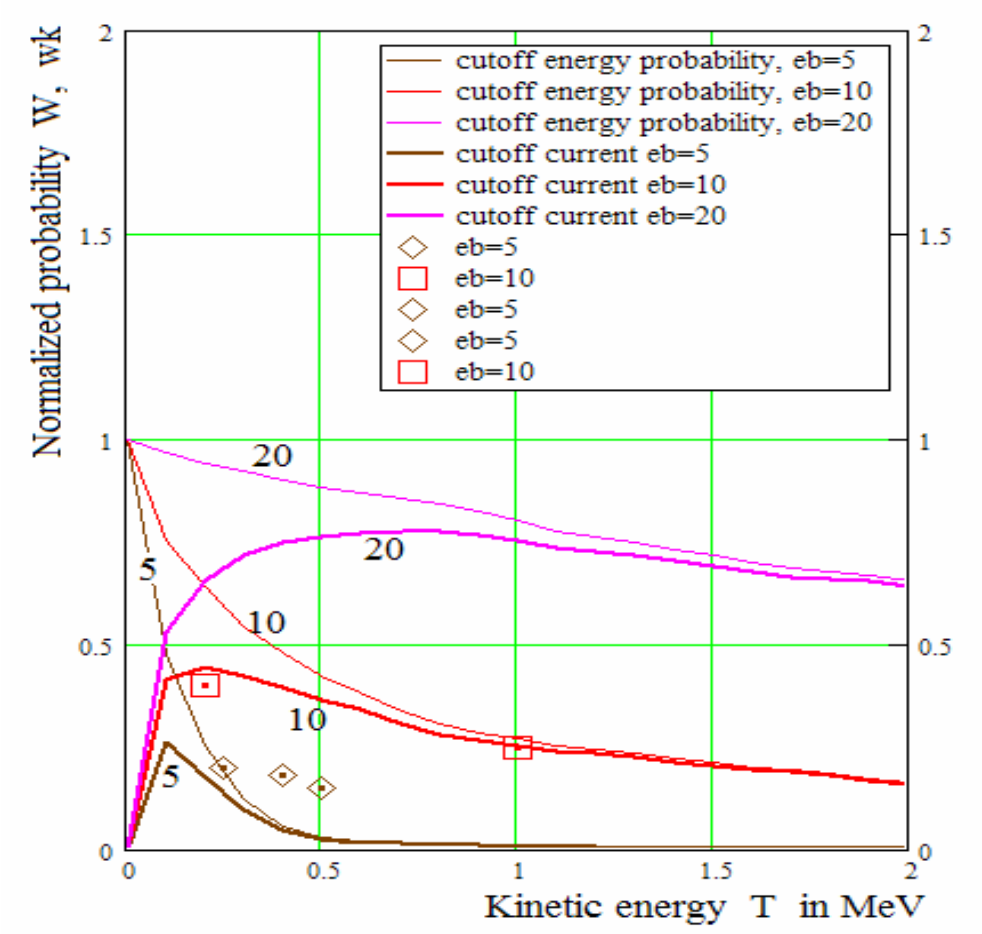

Fig.10. Comparison of simulation results with experimental data.

It is reasonable to consider the latter dependence as some effective characteristic "temperature" T_{eff} of hot electrons under stochastic acceleration. Within the range of intensities of $6\cdot10^{13}\div6\cdot10^{15}\,W/cm^2$ the dependence looks like $T_{eff}\sim q^{0.45\div0.55}$ at the wavelength $\lambda=1.06\,\mu m$. Within the range of intensities of $6\cdot10^{15}\div10^{17}\,W/cm^2$ the power increases $T_{eff}\sim q^{0.8\div0.9}$. Thus, as the intensity density approaches the relativistic one the power of this dependence becomes closer to unity.

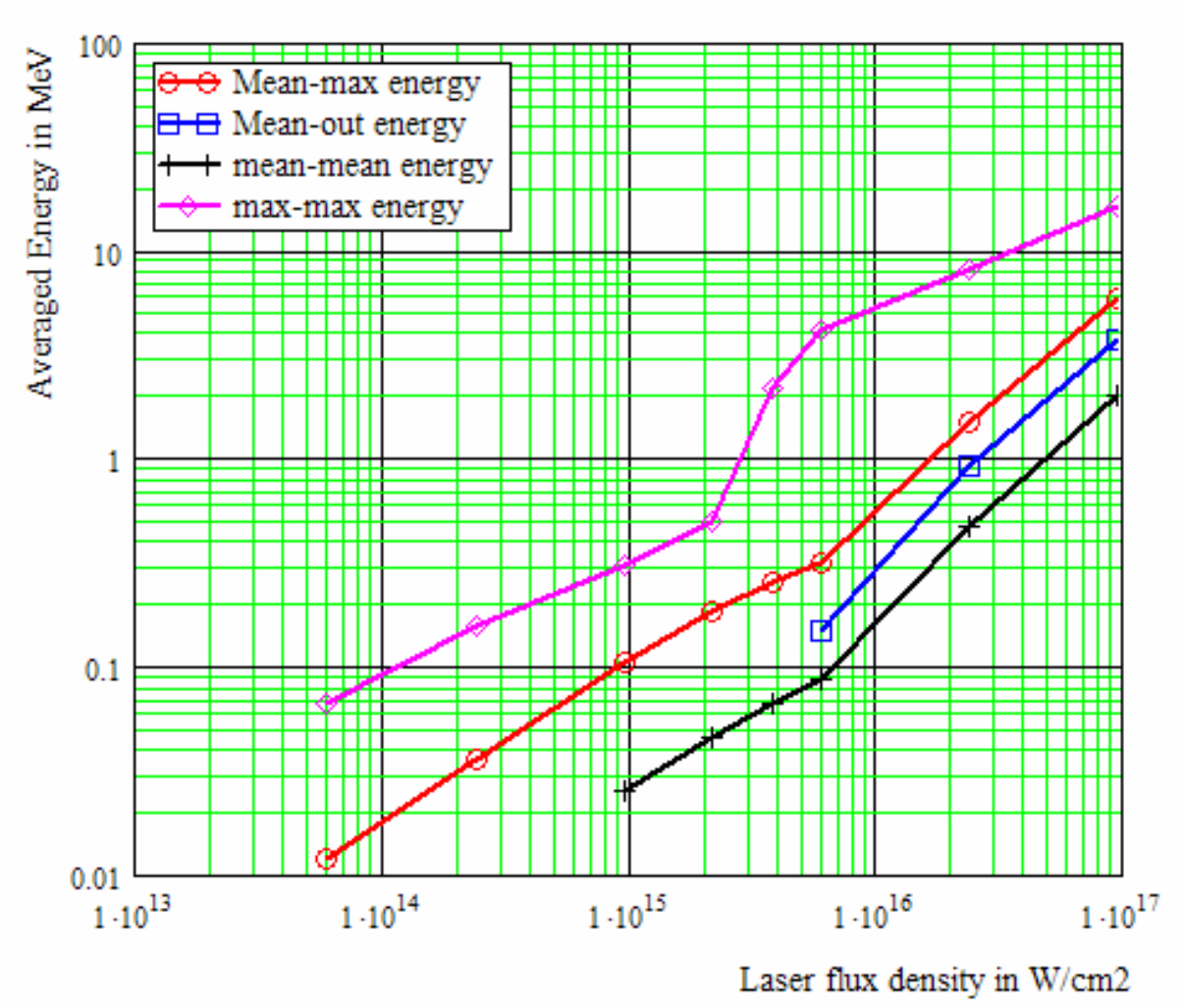

Fig.11. The dependence of maximal energy on the intensity (diamonds). The dependence of maximal energy on the intensity during the pulse averaged over 2000 electrons (circles). The averaged energy of electrons at the end of the pulse (boxes). The electron energy averaged over all electrons and averaged over the pulse for each electron (crosses).

Acknowledgements

Authors would like to thank V.V.Klimov and V.V.Okorokov for useful discussions.

References

[1] V.V.Ivanov, A.K.Knyazev, A.V.Kutsenko, A.A.Matsveiko, Yu.A.Mikhailov, V.P.Osetrov, A.I.Popov, G.V.Sklizkov, and A.N.Starodub, "Investigation of the generation of high-energy electrons in a laser plasma", JETP **82** (4), (1996), pp. 677-682.

V.V.Ivanov, A.K.Knyazev, N.E.Korneev, A.V.Kutsenko, A.A.Matsveiko, Yu.A.Mikhailov, V.P.Osetrov, A.I.Popov, G.V.Sklizkov, A.N.Starodub , "Method of fast electron observation in laser plasma", Prib. Tekn. Eksp. 4, (1995), p.77-81.

[2] M.H.Key, E.M.Campbell, T.E.Cowan, S.P.Hatchett, E.A.Henry, J.A.Koch, A.B.Langdon, B.F.Lasinski, A.MacKinnon, A.A.Offenberger, D.M.Pennington, M.D.Perry, T.J.Phillips, T.C.Sangster, M.S.Sing, R.A.Snavely, M.A.Stoyer, M.Tsukamoto, K.B.Wharton, S.C.Wilks, "The potential of fast ignition and related experiments with a petawatt laser facility", Journal of Fusion Energy, **17**, 3, (1998), pp.231-236.

[3] Zheng-Ming Sheng, Kunioki Mima, Jie Zhang, and Jurgen Meyer-ter-Vehn, "Efficient acceleration of electrons with counterpropagating intense laser pulses in vacuum and underdense plasma", Phys. Rev. E **69**, 016407, (2004), pp.1-12.

[4] Y.Sentoku, V.Bychenkov, K.Flippo, A.Maksimchuk, K.Mima, G.Mourou, Z.M.Sheng, D.Umstadter, "High-energy ion generation in interaction of short laser pulse with high-density plasma", Appl. Phys. **B74**, (2002), pp. 207-215.

[5] P.Zhang, N.Saleh, S.Chen, Z.M.Sheng, and D.Umstadter, "Laser-energy transfer and enhancement of plasma waves and electron beams by interfering high-intensity laser pulses", Phys.Rev.Lett., **91**, 22, (2003) 225001-1 – 225001-4.

[6] E.V.Maiorov, V.V.Okorokov, N.V.Sveshnikova, “On the acceleration of particles inside the static spatially inhomogeneous stationary electromagnetic field. Acceleration by inhomogeneous stochastic field”, Preprint 9-04 (2004) Inst. Theor. Exp. Phys., Moscow, pp.1-11.